2017

Hybrid model predictive control of a residential HVAC system with on-site thermal energy generation and storage

Massimo Fiorentini
University of Wollongong, massimo@uow.edu.au

Josh Wall
CSIRO

Zhenjun Ma
University of Wollongong, zhenjun@uow.edu.au

Julio H. Braslavsky
CSIRO, julio.braslavsky@csiro.au

Paul Cooper
University of Wollongong, pcooper@uow.edu.au

Publication Details

Fiorentini, M., Wall, J., Ma, Z., Braslavsky, J. H. & Cooper, P. (2017). Hybrid model predictive control of a residential HVAC system with on-site thermal energy generation and storage. Applied Energy, 187 465-479.

Hybrid model predictive control of a residential HVAC system with on-site thermal energy generation and storage

Abstract
This paper describes the development, implementation and experimental investigation of a Hybrid Model Predictive Control (HMPC) strategy to control solar-assisted heating, ventilation and air-conditioning (HVAC) systems with on-site thermal energy generation and storage. A comprehensive approach to the thermal energy management of a residential building is presented to optimise the scheduling of the available thermal energy resources to meet a comfort objective. The system has a hybrid nature with both continuous variables and discrete, logic-driven operating modes. The proposed control strategy is organized in two hierarchical levels. At the high-level, an HMPC controller with a 24-h prediction horizon and a 1-h control step is used to select the operating mode of the HVAC system. At the low-level, each operating mode is optimised using a 1-h rolling prediction horizon with a 5-min control step. The proposed control strategy has been practically implemented on the Building Management and Control System (BMCS) of a Net Zero-Energy Solar Decathlon house. This house features a sophisticated HVAC system comprising of an air-based photovoltaic thermal (PVT) collector and a phase change material (PCM) thermal storage integrated with the air-handling unit (AHU) of a ducted reverse-cycle heat pump system. The simulation and experimental results demonstrated the high performance achievable using an HMPC approach to optimising complex multimode HVAC systems in residential buildings, illustrating efficient selection of the appropriate operating modes to optimally manage thermal energy of the house.

Keywords
thermal, on-site, system, hvac, residential, energy, control, storage, hybrid, model, predictive, generation

Disciplines
Engineering | Science and Technology Studies

Publication Details
Fiorentini, M., Wall, J., Ma, Z., Braslavsky, J. H. & Cooper, P. (2017). Hybrid model predictive control of a residential HVAC system with on-site thermal energy generation and storage. Applied Energy, 187 465-479.

Hybrid model predictive control of a residential HVAC system with on-site thermal energy generation and storage

Massimo Fiorentini[1*], Josh Wall[2], Zhenjun Ma[1], Julio H. Braslavsky[2], Paul Cooper[1]

[1]Sustainable Buildings Research Centre (SBRC), Faculty of Engineering and Information Sciences, University of Wollongong, New South Wales, 2522, Australia

[2]Commonwealth Scientific & Industrial Research Organisation (CSIRO), CSIRO Energy Flagship, Newcastle, New South Wales, NSW 2304, Australia

*Corresponding Author: massimo@uow.edu.au

Abstract: This paper describes the development, implementation and experimental investigation of a Hybrid Model Predictive Control (HMPC) strategy to control solar-assisted heating, ventilation and air-conditioning (HVAC) systems with on-site thermal energy generation and storage. A comprehensive approach to the thermal energy management of a residential building is presented to optimise the scheduling of the available thermal energy resources to meet a comfort objective. The system has a hybrid nature with both continuous variables and discrete, logic-driven operating modes. The proposed control strategy is organized in two hierarchical levels. At the high-level, an HMPC controller with a 24-hour prediction horizon and a 1-hour control step is used to select the operating mode of the HVAC system. At the low-level, each operating mode is optimised using a 1-hour rolling prediction horizon with a 5-minute control step. The proposed control strategy has been practically implemented on the Building Management and Control System (BMCS) of a Net Zero-Energy Solar Decathlon house. This house features a sophisticated HVAC system comprising of an air-based photovoltaic thermal (PVT) collector and a phase change material (PCM) thermal storage integrated with the air-handling unit (AHU) of a ducted reverse-cycle heat pump system. The simulation and experimental results demonstrated the high performance achievable using an HMPC approach to optimizing complex multimode HVAC

systems in residential buildings, illustrating efficient selection of the appropriate operating modes to optimally manage thermal energy of the house.

Keywords: Hybrid model predictive control; Photovoltaic-thermal collectors; Phase change material thermal storage; Solar-assisted HVAC; System identification.

Nomenclature

A_i = equivalent area of internal solar gains [m^2]

A_e = equivalent area of wall solar gains [m^2]

c_p = specific heat of air [J/kg K]

C_i = indoor space equivalent capacitance [kWh/K]

C_e = effective thermal capacitance of walls [kWh/K]

C_{pcm} = effective capacitance of PCM unit [kWh/K]

$\overline{COP}$ = heat pump average coefficient of performance

$\delta_{m..}$ = discrete Boolean variables for operating modes

$\delta_{m..}$ = discrete Boolean variables for natural ventilation activation

δ_{hp} = discrete Boolean variable for heat pump activation

ε = cost associated to thermal comfort constraint softening [kW/°C]

η_{HP} = identifiable efficiency of the heat pump

Φ_{ig} = internal loads [kW]

Φ_{hp} = heat pump thermal generation [kW]

Φ_{PVT} = PVT system thermal generation [kW]

Φ_{PCM} = PCM unit thermal generation [kW]

Ψ = solar gains on building lumped capacitance surfaces [kW/m^2]

ρ = air density [kg/m^3]

R_{pcm} = equivalent PCM unit thermal resistance [K/kW]

R_w = equivalent half-wall resistance [K/kW]

R_v = equivalent infiltration resistance, operable windows closed [K/kW]

R_{vo} = equivalent infiltration resistance, operable windows open [K/kW]

T_a = ambient temperature [˚C]

$T_{pcm,i}$ = PCM unit inlet air temperature [˚C]

$T_{pcm,o}$ = PCM unit outlet air temperature [˚C]

T_i = average indoor temperature [˚C]

$\overline{T_i}$ = indoor temperature upper boundary [˚C]

$\underline{T_i}$ = indoor temperature lower boundary [˚C]

$T_{pvt,o}$ = PVT outlet temperature [˚C]

$T_{\mathrm{melt,b}}$ = PCM melting temperature, lower limit [˚C]

$T_{\mathrm{melt,t}}$ = PCM melting temperature, upper limit [˚C]

$\dot{V}$ = air volume flow rate [m^3/s]

1. Introduction

Increasing energy efficiency in buildings has been recognized as one of the fastest and most cost-effective means to save energy and reduce greenhouse gas emissions, as the building sector accounts for approximately 40% of the world's energy demand [1]. A central piece in improving building energy efficiency and sustainability is the installation, commissioning and fine-tuning of efficient Heating, Ventilation and Air Conditioning (HVAC) systems and Building Management and Control Systems (BMCSs) [2].

The concept of Net-Zero Energy Buildings (NZEBs), which capture the high-level of energy usage performance required from buildings, has received growing attention as a research and technology driver, and has been extensively discussed in many energy policy forums (e.g. [1]). An instrumental methodology in achieving the goal of a NZEB is the embedding of

optimal control strategies in building HVAC systems and BMCSs. These optimal control strategies can help match the building energy demand in face of weather-dependent energy generation and disturbances by efficiently integrating energy storage systems, which are now recognized as a proven demand management technology in building energy management.

However, the practical design and implementation of optimal control strategies that can efficiently integrate on-site energy generation and storage with a complex communication network between buildings, and to a smart grid, largely remains as a challenging problem [3]. Current industrial HVAC practice [4,5] is predominantly limited to the implementation of Rule-Based Control (RBC) and Proportional-Integral-Derivative (PID) control strategies, which have traditionally been reliable in the operation of building systems. However, such relatively simple classical control approaches cannot in general deal with the high performance requirements of modern buildings.

A proven advanced control strategy that can deal with such complex real-time optimal integration problem is Model Predictive Control (MPC). MPC is a well-established methodology in the control of complex interacting dynamic systems in the process industry, and has been receiving wide attention from the building control research community. In building systems, MPC has been applied to control the zone temperatures and building thermal mass [6–9], with numerous encouraging experimental results reported [10]. The formulation of dynamic models, a critical component of the MPC strategy, has been undertaken in a number of building studies [11,12], based on identifiable models and the use of model parameter identification techniques [13–16].

MPC has also been used to solve on-site generation and storage scheduling problems [17,18] with continuous variables and discrete, logic-driven operating modes, generally leading to a mixed–integer programming problem to be solved [19,20]. This is commonly referred as Hybrid MPC (HMPC) [21–23].

In the area of residential buildings, implementation of MPC on a conventional heating system showed a significant increase in the system energy efficiency [24]. A comprehensive framework based on an MPC algorithm was presented by Di Giorgio and Liberati [25] to optimally schedule electrical generation, storage and controllable demand in a house.

Many modern residential buildings, which are often aiming to achieve the Net Zero-Energy target, implement renewable technologies on their HVAC systems, where the coordination of solar thermal generation, thermal energy storage, conventional air conditioning systems and operable windows must be optimally controlled to achieve efficiency and thermal comfort objectives.

While quite extensive work has been undertaken in optimising temperature control or scheduling electrical resources in buildings using the MPC framework, to the best of the authors knowledge, there is a gap in current research in developing a comprehensive MPC framework for this typology of HVAC systems at a residential scale, as well as a lack of experimental demonstrations of their operation. Since these thermal energy resources are highly weather-dependent, it is believed that these systems could strongly benefit from the application of an MPC approach, through optimising the building thermal dynamics with the management of the renewable and conventional thermal energy resources. As the optimisation problem to be solved features a combination of continuous and discrete dynamics, this will lead to the formulation of an HMPC controller. A preliminary investigation on the application of an MPC strategy on the system studied in this paper showed some promising results [26].

In this paper, an HMPC strategy is developed for optimising the operation of a solar-assisted HVAC system, which includes Photovoltaic-thermal (PVT) collectors, an active PCM thermal storage unit, a conventional reverse cycle air conditioning unit and operable windows implemented in the ‘Illawarra Flame’ house, a net zero-energy retrofit house that won the

Solar Decathlon China 2013 Competition. The system was designed for operation during both winter and summer, using daytime solar radiation and night sky radiative cooling to increase overall energy efficiency. To compute a near-optimal solution for this type of system [27], the problem formulated as a Mixed Logical Dynamical (MLD) model can capture both continuous and discrete dynamics, for which an HMPC controller is then developed.

In this study, an R-C model was utilised to represent the house dynamics and a system identification of the key parameters was performed using the experimental data collected from the house operation. A hierarchical HMPC control structure was implemented in Matlab using the Hybrid Toolbox for Matlab [28]. A key objective of this study was to experimentally demonstrate the implementation of this HMPC controller. A live communication link between the Matlab script and the BMCS of the 'Illawarra Flame' house allowed the deployment of the real-time controller and its testing on the real system. Section 2 describes the case study HVAC system and its control system, followed by the description of the grey-box building model and its identification in Section 3. The description of the HVAC system models is provided in Section 4 and the MPC formulation is presented in Section 5. The experimental results are reported in Section 6 and the conclusion is provided in Section 7.

2. Description of the case study HVAC System and Operating Modes

The Team UOW Solar Decathlon house, its automated windows, and the schematic of its HVAC system are shown in Figure 1. This HVAC system integrates a number of energy components including a PVT system, a PCM thermal storage and a conventional air conditioning system with an outdoor condenser unit and an indoor air-handling unit (AHU). The PVT is used to generate the electricity and the low-grade thermal energy. The PCM storage is used to store the low-grade thermal energy, which may then be used later for space heating or cooling. The thermal storage is 'charged' by warm or cool air generated from the

PVT either by winter daytime solar radiation or summer night-time sky radiative cooling, respectively.

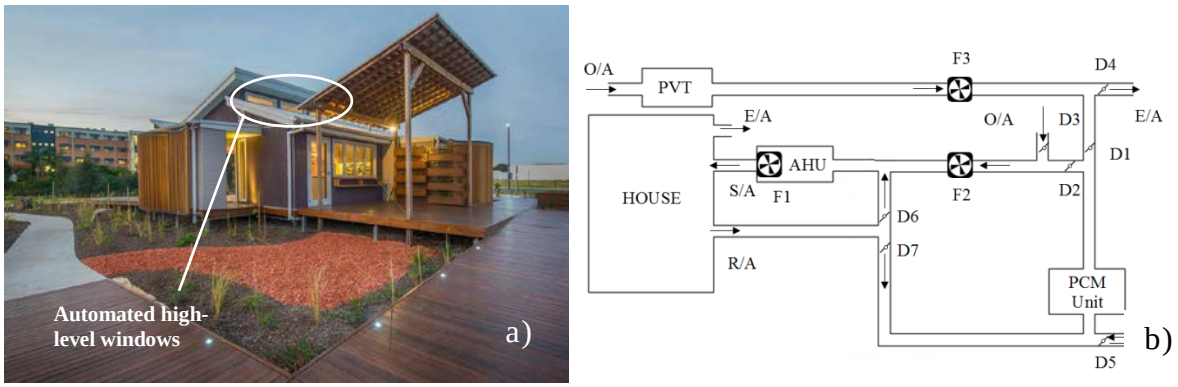

Figure 1: a) Team UOW Solar Decathlon house and its automated high-level windows and b) Schematic of the solar-assisted HVAC system where the symbols represent the following: S/A supply air, O/A outside air, R/A return air, E/A exhaust air, F fan and D damper, respectively

There are five operating modes in this HVAC system, including three conditioning modes and two PVT modes, which are controlled through the BMCS specifically designed for the house.

Conditioning modes

Depending on the indoor conditions, the system can either work in the 'natural ventilation' mode through automatically controlling the opening of the high-level windows, or work in the mechanical heating mode or mechanical cooling mode. Selection of the three conditioning modes is determined based on the measured indoor and outdoor conditions.

In the mechanical heating and cooling modes, the system can operate in three different sub-modes, i.e. *Direct Photovoltaic-Thermal Supply, Supply Air Preconditioned through Phase Change Material, and Normal Heating and Cooling Mode.*

PVT modes

If there is no interfering operating mode activated, the system can operate in two other modes, including *PCM Charging and PVT Exhaust.* A detailed description of the operating

modes for the HVAC system can be found in [26]. The mode of *PVT Exhaust* is not considered in this study.

2.1 BMCS Description and System Integration

The control system of the Illawarra Flame house was designed to accommodate the objectives and constraints of the overall project, capable of controlling lighting systems, operable windows and the complex HVAC system. The BMCS system designed is also to be capable of monitoring temperatures, energy consumption, electricity generation and flow rates, and can effectively report this information to the user via a graphical interface. For sourcing and project sponsoring reasons, the Australian manufacturer and supplier Clipsal, and its proprietary building management and control system C-Bus were used in the project.

A supervisory BMCS (Tridium Niagara JACE) was integrated with the C-Bus system because of its capability to utilize various communication languages and the availability of drivers for common C-Bus units. This allowed a successful integration of the system components on for example Modbus and oBIX [30] networks. The JACE controller acts as a supervisor, informing C-Bus on which mode the system should operate and controlling the associated variables.

The JACE controller is also given the capability of overriding the local controller of the reverse-cycle air conditioning unit, utilising a Modbus gateway. This allows the control system to dynamically change the operation mode of the HVAC system, temperature set-point and fan speed.

In order to easily implement the Hybrid MPC strategy, a machine running the Hybrid MPC Matlab script is necessary, with the possibility to real-time override the JACE Niagara data points. The Matlab script was interfaced to the JACE controller using an oBIX network interface developed by the researchers from the Newcastle Energy Centre, Commonwealth Scientific & Industrial Research Organisation (CSIRO). This facilitates the implementation

of virtually any desired control strategies in the house. The solver utilised for the optimisation was Gurobi [31]. The HMPC controller was implemented on a commercial laptop computer with an Intel® Core™ i5 Processor (2.7GHz).

2.2 Control Chain Structure

Given the complexity of the problem to be solved, the HMPC control strategy was divided into a high-level HMPC controller and multiple low-level HMPC controllers. The information collected from the weather station is used for the weather forecast and the prediction of the future PVT outlet temperature and its potential useful thermal generation together with the system states, which are then used to compute the optimal control action generated by the HMPC. The first set of actions from the optimal control sequence is then sent to the BMCS to control the individual components and HVAC equipment.

The objective of the high-level HMPC is to compute the optimal sequence of the operating modes, using a control step of 1 hour and a prediction horizon of 24 hours.

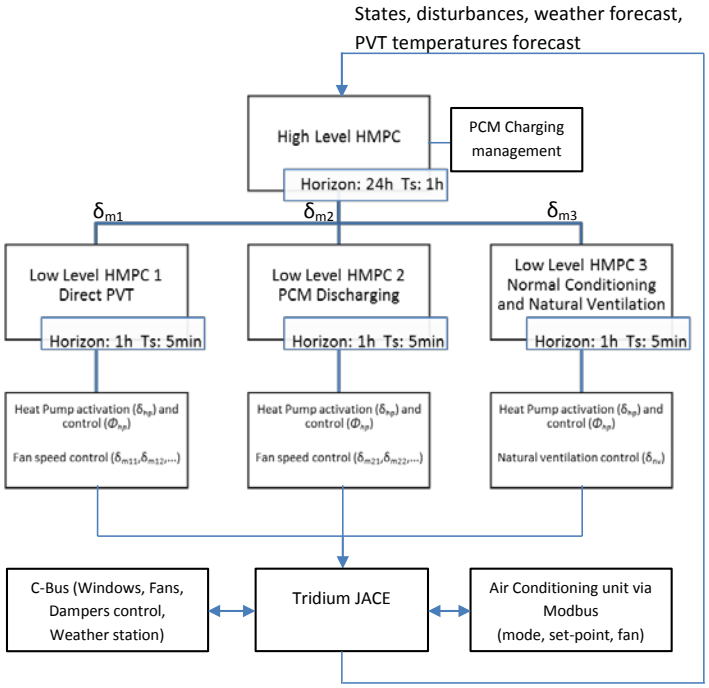

Figure 2: Control chain structure: the high-level controller selects the Conditioning mode and manages the PCM Charging mode and; the low-level controllers optimise the Conditioning mode and control the system.

Once the high-level HMPC has selected the operating mode for the next hour, the corresponding low-level HMPC controller is then activated (Figure 2). The objective of each low-level HMPC controller is to optimise the selected operating mode for the time period of concern, considering the range of the fan speeds that can be utilized for the PVT and PCM storage, for example. The low-level HMPC computes the optimal solution with a control step of 5 minutes and a prediction horizon of 1 hour. Once the optimal sequence of control actions has been computed, the first set of the actions is then sent to the JACE controller and applied to control the operation of the HVAC system (Figure 2).

2.3 Measurement Instrumentation

The weather conditions, including ambient temperature, solar radiation, and wind speed and direction, were monitored using a Davis Vantage Pro II Weather station and integrated through an RS232 connection to the C-Bus and JACE control units. Air flow rate was monitored using Siemens QVM62.1 air velocity sensors, located at one-third of the duct diameter from the duct centreline. These sensors had a stated accuracy of ±0.2 m/s + 3% of the measured values. The temperatures in the ductwork were measured using Clipsal C-Bus Digital Temperature Sensor Units 5104DTSI with a stated accuracy of ±0.5°C in the temperature range of -10-80°C.

3. Building Modelling and System Identification

The HMPC control strategy is developed based on a grey-box state-space model. The model, based on an R-C analogy, was developed in a similar manner to identifiable models available in the literature [13]. The parameters of this model were estimated using the datasets of the system in its various configurations, forcing the building with intermittent heating or cooling, and using the average temperature (from five temperature sensors) of the building as the thermal response. The building was therefore treated as a single thermal zone. The estimation of the building parameters was performed using a nonlinear least-square fitting method.

The building was originally set to operate in two main modes, i.e. mechanical ventilation when the high-level windows were completely closed and natural ventilation when the high-level windows were fully open. In order to keep the system linear and easily identifiable, natural ventilation was simply modelled with different building infiltration rates, i.e. R_v when the windows are closed and R_{vo} when the windows are open. The R-C model of the building is presented in Figure 3.

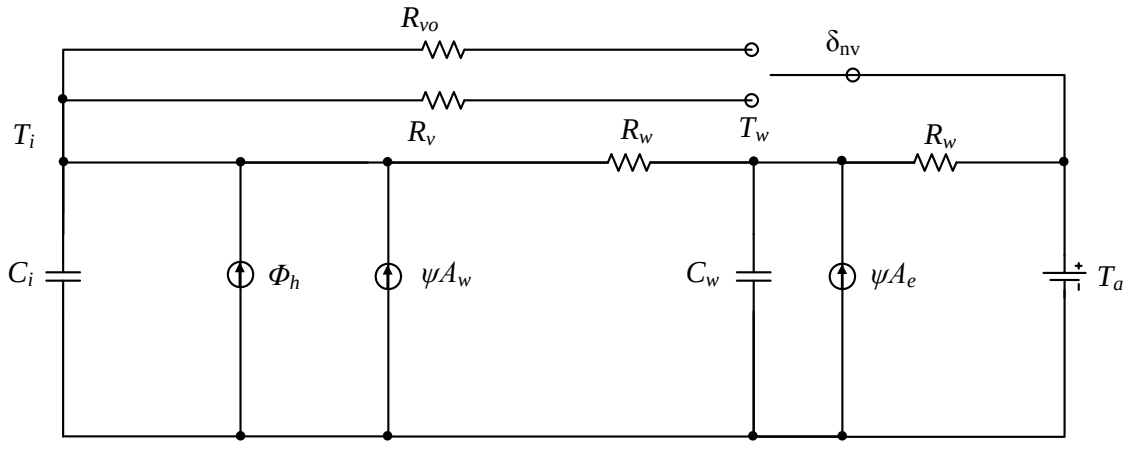

Figure 3: R-C representation of the building thermal system.

In this model, the state vector is $x = [T_i, T_w]^T$, and the input vector is $u = [T_a, \Psi, \Phi_h]^T$. The Boolean switch δ_{nv} represents the opening of the windows.

The parameters subject to identification are the equivalent half wall resistance R_w, the infiltration equivalent resistance with the windows closed R_v, the infiltration equivalent resistance with windows open R_{vo}, the equivalent internal capacitance C_i, the equivalent wall capacitance C_w, the equivalent windows area A_w, and the equivalent external wall area A_e.

The system dynamics are described by the state-space equations of the R-C model illustrated in Figure 3.

3.1 Identification of the House Parameters

The model parameters, which represent the physical characteristics of the building, were identified using a number of datasets obtained from the real operation of the building, where the indoor temperature was forced to intermittently use the PVT system or the heat pump

system. When the PVT system is active, the heating introduced to the building is calculated as

$$\Phi_{h\_PVT} = \rho \dot{V} c_p \left(T_{pvt,o} - T_i\right) \quad (1)$$

When the heat pump system is active, the heating or cooling input of the heat pump, which is not directly measurable in the house setup, is considered to be proportional to the electrical consumption of the air conditioning unit ($\Phi_{c,el}$), following the relationship

$$\Phi_{h\_HP} = \eta_{HP} \overline{COP} \Phi_{c,el} \quad (2)$$

In this study, a constant COP was considered to simplify the control problem, as the main objective of the controller is to optimise the operation of the whole system.

Three input datasets were used for this identification, including the data with intermittent heating of the building with the heat pump, intermittent heating with the PVT system and cooling with the heat pump. An example is presented in Figure 4a, where the data set used and the responses of the building are presented, in the case of the heating with the heat-pump test.

a)

b)

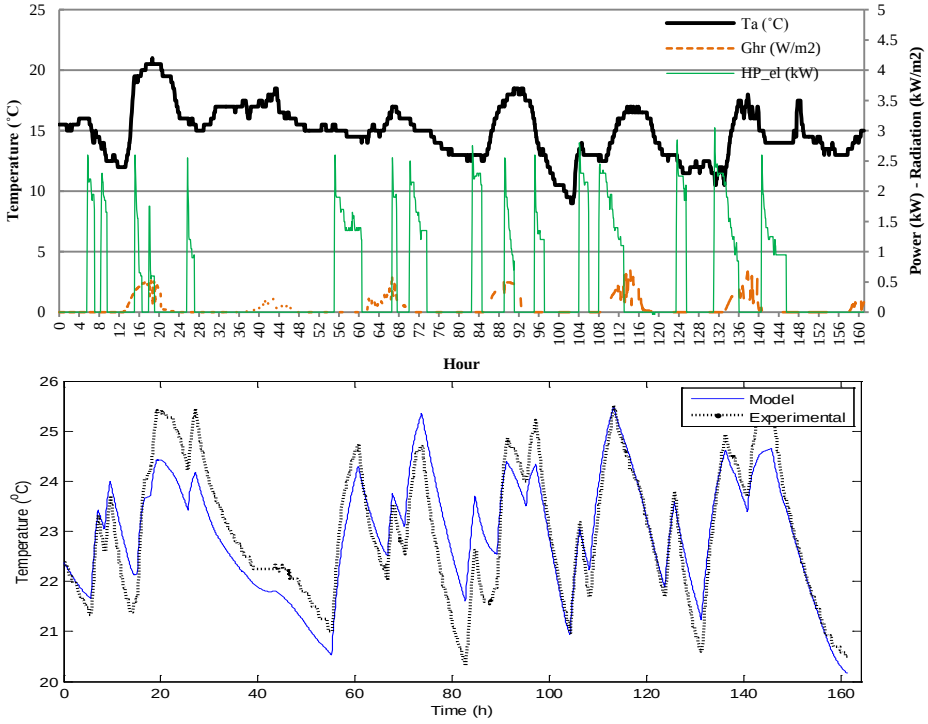

Figure 4: a) Identification input data heating with heat pump where *HP_el* is the electrical consumption and b) comparison between the data from the identified model and experimental data.

As the proposed model is linear and time-invariant, Matlab's System Identification Toolbox in-built linear grey-box model estimation function [32] was used to fit the model parameters using the experimental data.

To ensure that the values of the parameters identified are representative to the physical lumped resistances and capacitances, the 'first guess' and boundary conditions were chosen based on the design values of the Illawarra Flame house and commonly used minimum and maximum design values for each parameter. The values used are summarized in Table 1.

Table 1: Building parameters identification

Parameter	First Guess	Lower Boundary	Upper Boundary	Identified Value
R_w (K/kW)	7.90	2	20	6.54
C_i (kWh/K)	0.76	0.06	5	3.39
C_w (kWh/K)	22	1	40	6.72
A_e (m^2)	20	0.50	50	2.91
A_w (m^2)	1	0.01	5	1.15
R_v (K/kW)	7	1	20	7.62
η_{HP}	0.90	0.60	1	0.61

The comparison between the measured response and the predicted response of the identified system under the three operation conditions is shown in Figure 4b.

The goodness of fit between the measured and the predicted outputs, widely used metric, defined in the Matlab System Identification Toolbox and [33], was 48.38, 54.15 and 57.48% for the three different operation conditions, respectively.

The procedure was repeated for the natural ventilation mode to identify infiltration equivalent resistance with the windows open R_{vo}. To quantify this parameter, a test was conducted where the operable windows were kept fully open for a week, leaving the house free-running. The boundaries for the parameter R_{vo} were the same as for R_v in the identification with the windows closed. The identified infiltration equivalent resistance was 3.28, which is less than half of the infiltration resistance with the windows closed.

The goodness of fit between the both sets of the data was 47.09%. The results of these identifications can therefore be considered acceptable [11], considering that natural

ventilation was also included, the limitations of the model (e.g. no influence of wind speed and direction on R_{vo}), the fact that multiple sources of thermal energy were used, the relatively limited inputs available from the measurements available to the building model, and the uncertainty associated with the experimental tests. While the statistical goodness of fit of the identified model in the open loop is around 50%, due to measurement noise and disturbances, it is evident from Figure 4b that the model captures the dominant system dynamics, which is acceptable for control purposes. This observation is further supported by the closed-loop performance of the system, presented in Sections 6.1 and 6.2.

4. Modelling of Solar-PVT Assisted HVAC System

4.1 PVT System and PVT Direct Supply

The PVT collector studied in this paper consists of a number of thin-film PV panels mounted on a steel sheet flashing that is fixed onto the top of an existing sheet metal roof profile. This system creates a cavity underneath the steel flashing through which the air exchanges heat with the PVT panels.

To describe the heat transfer in the PVT, a steady-state model was employed to derive an analytical solution to determine the PVT output [29]. The calculated outlet temperature of the PVT is then used to calculate the heating that the PVT system can supply to the building using Eq. (1).

4.2 PCM Thermal Storage unit and PCM Discharging

The PCM thermal storage unit in the Solar Decathlon house was designed to exchange the heat between the PCM and the air. It consists of PlusIce PCM bricks [34], which were placed vertically and spaced to create the channels for the air to flow through. The phase change temperature of the material used is 22˚C. The relationship used to describe the heat exchange in this PCM unit was presented in Ref. [29].

The heating that the PCM storage unit can supply to the building is determined by the equation

$$\Phi_{h\_PCM} = \rho \dot{V} c_p (T_{pcm,o} - T_i) \quad (3)$$

The equivalent thermal capacitance of the PCM unit was calculated through interpolating the differential scanning calorimeter test data measured at the Fraunhofer - Institut Für Solare Energiesysteme in Freiburg. The equivalent thermal capacitance was divided into three ranges, including the solid range ($C_{pcm,s}$), the phase change range ($C_{pcm,c}$), and the liquid range ($C_{pcm,l}$).

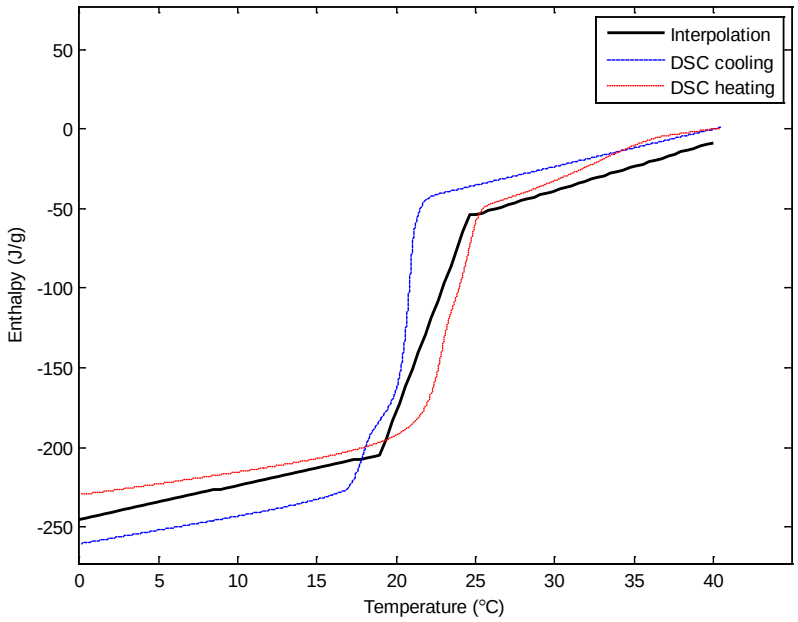

Figure 5: PCM equivalent thermal capacitance tested under a cooling and heating rate of 0.01K/min and a temperature range of 0-40°C.

The equivalent capacitances of the PCM were 0.40, 5.10 and 0.57kWh/°C for the solid range, the phase change range and the liquid range, respectively.

The curve used for the implementation in the HMPC system is represented in Figure 5.

4.3 PCM Charging with PVT

In the PCM charging with PVT, the total heat stored in the PCM unit can be determined by the equation

$$\Phi_{h\_Charged} = \rho \dot{V} c_p \left(T_{pvt,o} - T_{pcm,o}\right) \quad (4)$$

4.4 Energy Consumption of the System Components

The energy consumption of the system components in each operating mode is needed to compute the optimal solution of the controller to allocate a cost for each energy source.

Identification of the electrical consumption versus the air flow characteristics was the key aspect of the optimisation of the operating modes involving the PVT system or the PCM unit. The fit used was a 3rd order polynomial of the form

$$P_{fan} = \gamma_D \, \dot{V}^3 \quad (5)$$

where the coefficient γ_D is related to the system pressure losses and is calculated for each operating mode. The identification of these curves was presented in [35]. In this study, the consumption-airflow characteristic was considered at the discrete fan speed levels.

The energy used by the heat pump is instantaneously measured and represented by $\Phi_{c,el}$. The energy used in the natural ventilation mode is considered negligible and an infinitesimally small energy cost was associated to its operation.

5 Hybrid Model Predictive Control Development

The HVAC system presented in this study can operate in three different conditioning modes and one PVT mode. The switching between these operating modes would indicate a system model with a time-varying structure. The switching is also constrained, since some of these modes cannot operate simultaneously (e.g. PCM Charging and PCM Discharging modes) due to the physical constraints. Furthermore, the relationships between the PVT outlet temperature and the airflow rate are intrinsically nonlinear.

The switching and nonlinearity issues described above may be tackled by approaching the MPC problem formulation as an HMPC problem. HMPC can deal with both continuous and discrete dynamics, seeking optimal solutions by solving a mixed-integer programming problem. In particular, it is possible to describe this problem as a Mixed Logical Dynamical

(MLD) system, in which the logic, dynamics and constraints are integrated as described in [27,28].

Taking into account the future samples of the reference vector and measured disturbance, the prediction model has to be augmented with an additional linear model and treat the vector of the future references and measured disturbances as the additional states [36].

Writing the problem as an MLD system with the discrete fan speeds removes the difficulty of the aforementioned problems. Indeed, this results in a number of linear systems that can be activated by appropriate Boolean variables. For each of these linear systems, the cost is fixed at the energy used by the fan with the selected discrete speed step with the addition of the consumption of the heat pump.

Given the number of Boolean variables and the requirement to compute the solution in a relatively short time period (e.g. 5 minutes), the controller was divided into two levels: a high-level controller that selects the operating mode every hour, and three low-level controllers that optimize the operation of each operating mode every five minutes.

Each controller will have to minimise a cost function of the form

$$min_{\{u,d,z\}_0^{N-1}} J(\{u,d,z\}_0^{N-1}, x(t)) \triangleq \sum_{k=1}^{N-1} \|Q_x(x(k) - x_r)\|_p + \sum_{k=1}^{N-1} \|Q_u(u(k) - u_r)\|_p + \sum_{k=1}^{N-1} \|Q_z(z(k) - z_r)\|_p + \sum_{k=1}^{N-1} \left\|Q_y(y(k) - y_r)\right\|_p + \|Q_{xN}(x(N|t) - x_r)\|_p \quad (6)$$

The values and the parameters included in the cost function vary from controller to controller. For this study, the infinity norm was used, with $p = \infty$.

5.1 High-Level Controller

The main purpose of the high-level controller (Figure 6) is to determine the system operating mode under a given working condition. To maintain the problem relatively simple and minimise the number of Boolean optimisation variables, each mode was considered to operate at its nominal conditions (e.g. the fan speed for PVT Direct Supply and PCM Charging mode is considered to be at 80% of the VSD range, corresponding to a flow rate of approximately 300 L/s).

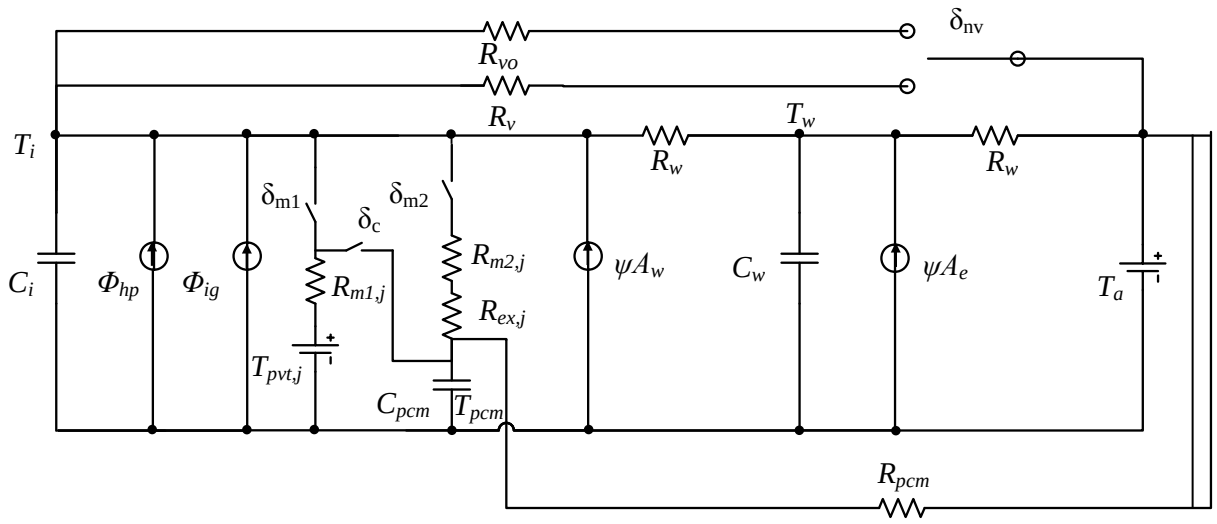

Figure 6: Schematic of High-level Controller system.

The states of the high-level controller, the measured disturbances and the controlled variables are summarised in Table 2. The resistances R_{m1j} and R_{m2j} represent the delivered heating and cooling to the building using the nominal air mass flow rates in PVT Direct Supply and PCM Discharging modes, respectively. $R_{ex,j}$ represents the heat exchange rate of the PCM unit at the nominal air flow rate. The equivalent PCM capacitance C_{pcm} at each time step k is defined as

$$C_{pcm}(k) = \begin{cases} C_{pcm,s} & if \quad T_{pcm} < T_{melt,b} \\ C_{pcm,c} & if \quad T_{melt,b} \le T_{pcm} \le T_{melt,t} \\ C_{pcm,l} & if \quad T_{pcm} > T_{melt,t} \end{cases} \tag{7}$$

Once the high-level controller has selected the operating mode for the next hour, one of the low-level controllers will be activated. The objective of this controller is to track the reference temperature given by the high-level controller, using the next computed state of the average indoor temperature T_i. The states of the low-level controllers, the measured disturbances and the controlled variables are also summarised in Table 2.

Table 2: HMPC states, measured disturbances and controlled variables.

Items	Parameters	Description	High-level	Low-level 1	Low-level 2	Low-level 3
States	T_i	average inside temperature (measured)	✓	✓	✓	✓
	T_w	equivalent wall temperature (estimated)	✓	✓	✓	✓
	T_{pcm}	average PCM temperature (measured)	✓	×	✓	×
Measured disturbance	T_a	ambient temperature	✓	✓	✓	✓
	Ψ	global horizontal radiation	✓	✓	✓	✓
	Φ_{ig}	Internal loads	✓	✓	✓	✓
	$T_{pvt,j}$	PVT calculated outlet temperature at fan speed *j*	✓	✓	×	×
Controlled variable	ε	constraint softening on indoor temperature	✓	×	×	×
	Φ_{hp}	thermal input to the building provided by the heat pump	✓	✓	✓	✓
	δ_{m1j}	PVT Direct Supply (at fan speed *j* in low-level controllers)	✓	✓	×	×
	δ_{m2j}	PCM Discharge Supply (at fan speed *j* in low-level controllers)	✓	×	✓	×
	δ_c	PCM Charging mode	✓	×	×	×
	δ_{nv}	Natural ventilation mode	✓	×	×	✓
	δ_{hp}	Heat pump active (minimum heat delivery)	×	✓	✓	✓

The set of the constraints associated with the high-level controller are as follows:

- Two conflicting modes are not activated at the same time;
- The heat pump thermal input respects the physical limits of the real unit; and
- The comfort conditions are maintained, keeping the average indoor temperature in the defined comfort range.

The limit of the air conditioning thermal capacity (Φ_{hp}) is represented by $[\overline{\Phi_{hp,}}\ \underline{\Phi_{hp}}]$, and the limits of the allowance for the temperature to go outside the comfort band (ε) is represented by $[\overline{\varepsilon}, \underline{\varepsilon}]$. The logical conditions are:

$\sim(\delta_{m2} \,\&\, \delta_{m1})$, $\sim(\delta_{m2} \,\&\, \delta_{nv})$, $\sim(\delta_{m1} \,\&\, \delta_{nv})$, $\sim(\delta_{m2} \,\&\, \delta_{c})$, $\sim(\delta_{m1} \,\&\, \delta_{c})$, $T_i <= \overline{T_i} + \varepsilon$, $T_i >= \underline{T_i} - \varepsilon$.

Where ~ is the "not" condition and & is the "and" condition.

5.2 Low-Level Controller 1 – Direct PVT and Normal Conditioning

Low-level controller 1 (Figure 7) is selected when the Boolean variable δ_{m1} of the high-level controller is active. This controller sets the system in mechanical ventilation and operates the PVT Direct Mode in conjunction with the operation of the heat pump. This controller can select various Boolean variables corresponding to the discrete fan speed levels.

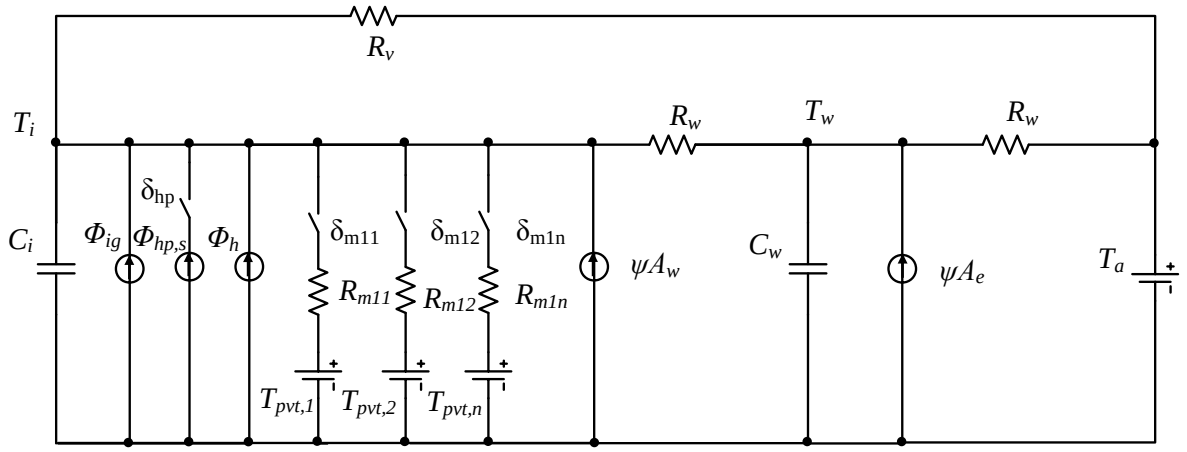

Figure 7: System schematic of low-level controller 1.

The PVT system can provide the thermal energy independently or can operate in conjunction with the heat pump (PVT Direct mode and PVT pre-heating/pre-cooling the air for the AHU). The heat pump can also operate without the PVT (Normal Conditioning mode).

The resistances $R_{m11,}$ $R_{m12,}$ R_{m1n} represent the heating/cooling delivery to the building using the various air mass flow rates.

The set of the constraints associated to the low-level controller 1 are as follows:

- Two fan speeds are not activated at the same time;

- The heat pump thermal input respects the physical limits of the real unit; and
- The comfort conditions are maintained, following the trajectory defined by the high-level controller.

The limits of the air conditioning thermal capacity (Φ_{hp}) are the same as that of the high-level controller. Logical conditions are:

$\sim(\delta_{m11} \,\&\, \delta_{m12})$, $\sim(\delta_{m11} \,\&\, \delta_{m1n})$,…, $\sim(\delta_{m12} \,\&\, \delta_{m1n})$, $\sim(\delta_{hp} \,\&\, \Phi_{hp} \neq 0)$..

5.3 Low-Level Controller 2 – PCM Discharging and Normal Conditioning

Low-level controller 2 (Figure 8) is selected when the Boolean variable δ_{m2} of the high-level controller is active. This controller sets the system in mechanical ventilation and operates the PCM Discharging Mode in conjunction with the operation of the heat pump. This controller can select various Boolean variables that correspond to the discrete fan speed levels.

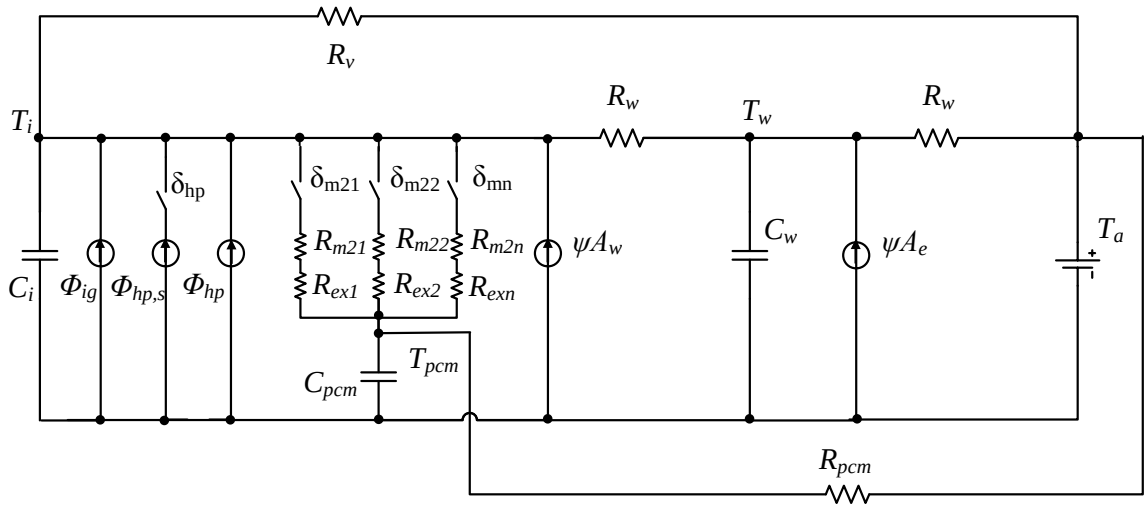

Figure 8: System schematic of low-level controller 2.

The resistances $R_{ex1,}$ $R_{ex2,}$ R_{exn} represent the heat exchange rate into the PCM unit corresponding to the various air flow rates and $R_{m21,}$ $R_{m22,}$ R_{m2n} represent the heating and cooling delivery to the building using the various air mass flow rates.

The set of the constraints associated to the low-level controller 2 are similar to the ones of the low-level controller 1.

$\sim(\delta_{m21} \,\&\, \delta_{m22})$, $\sim(\delta_{m21} \,\&\, \delta_{m2n})$,…, $\sim(\delta_{m22} \,\&\, \delta_{m2n})$, $\sim(\delta_{hp} \,\&\, \Phi_{hp} \neq 0)$.

5.4 Low-Level Controller 3 – Natural Ventilation and Normal Conditioning

Low-level controller 3 (Figure 9) is selected when neither the Boolean variable δ_{m1} nor δ_{m2} of the high-level controller are active. This controller sets the mechanical ventilation system Normal Conditioning Mode and operates the heat pump depending on the value of the optimal thermal input Φ_{hp} calculated at each control step, and operates the high-level operable windows of the house. This controller utilises two Boolean variables that correspond to the operation of the building in mechanical or natural ventilation and the activation of the heat pump.

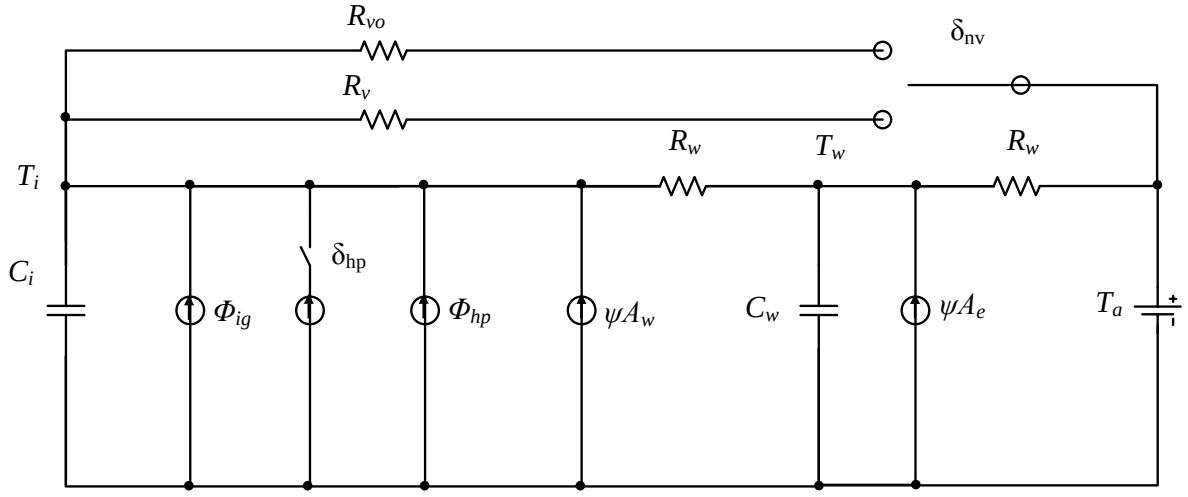

Figure 9: System schematic of low-level controller 3.

The set of the constraints associated to the low-level controller 3 are as follows:

- Natural ventilation and air conditioning are not to be activated at the same time;
- The heat pump thermal input respects the physical limits of the real unit; and
- The comfort conditions are maintained, following the trajectory defined by the high-level controller.

The limits of the air conditioning thermal capacity (Φ_{hp}) are the same as that of the high-level controller. The logical conditions are that natural ventilation and the air conditioning do not operate at the same time and the heat pump cannot provide additional heating if it is not switched on.

469 $\sim(\delta_{hp} \,\&\, \delta_{nv})$; $\sim(\delta_{hp} \,\&\, \Phi_{hp} \neq 0)$.

470 Given the objective of the low-level controllers, it is possible that the controller will
471 intermittently heat and cool the building to follow a certain trajectory. To avoid this problem,
472 each low-level controller was developed in two versions, i.e. one only allows heating and the
473 other only allows cooling. The type of the controller used is dictated by the request for
474 heating or cooling by the high-level controller and for that hour the appropriate low-level
475 controller is selected.

476 **5.5 Weather Forecast**

477 In this paper, an adaptive weather-prediction model developed in [37] was used to forecast
478 external dry-bulb temperature and solar radiation over the 24 hours prediction horizon. These
479 predictions serve as the inputs to both the building model and the PVT analytical thermal
480 model.

481 Among the various approaches presented in [37], the Deterministic-Stochastic method was
482 adopted to predict both external dry-bulb temperature and solar radiation.

483 **6 Experimental and Simulation Results**

484 The experiments were conducted using the Illawarra Flame house at Innovation Campus,
485 Wollongong, in March and April 2015. The two tests were carried out using the HMPC
486 strategy presented in this paper, mainly in cooling dominated periods. In the first test, only
487 mechanical ventilation was used, while in the second one natural ventilation was also
488 included. Tests were also conducted during the heating dominated periods, but the results are
489 not presented in order to avoid a lengthy paper. Difficulties in implementing the target R=3.0
490 insulation to the PCM storage unit could not be fully achieved, and therefore affected the
491 PCM heat loss. The HMPC strategy successfully controlled the system, despite the issues
492 with the real system.

493 The tests were performed using a variable comfort band, which was considered as a variable
494 soft constraint for the average indoor temperature, where the upper boundary $\underline{T_i}$ and the
495 lower boundary $\overline{T_i}$ for the cooling and heating are defined as

496 $$\overline{T_i}(k) = \begin{cases} 24°C & if\ 9 \le hour(k) \le 18, \\ 25.5°C & otherwise. \end{cases} \quad (8)$$

497 $$\underline{T_i}\,(k) = \begin{cases} 20°C & if\ 9 \le hour(k) \le 18, \\ 18.5°C & otherwise\,. \end{cases} \quad (9)$$

498 Once the tests were completed, the same weather data was then used in a simulated
499 environment in which the models of the building and equipment were the same as those
500 previously presented.
501 The simulated controller has to deal with the same mismatch in the weather prediction, but
502 there is no mismatch between the model used in the HMPC controller and the controlled
503 system.

504 **6.1 Cooling Test - Mechanical Ventilation Only**

505 This test was conducted between 6th and 11th of March 2015. To stay within the defined
506 comfort band, cooling was mostly required. The experimental and simulated indoor
507 temperature profiles, outdoor temperature, global horizontal radiation and the objective
508 temperature range are presented in Figure 10. In this test the daytime comfort band ended at
509 5pm instead of 6pm. One can notice that both the simulated and experimental controllers led
510 to the similar indoor temperature profiles, where it is noticeable the attempt to pre-cool the
511 building at the end of the night, and drift as much as possible inside the comfort band. The
512 reason behind this choice of the HMPC controller is that the most efficient cooling generation
513 came from the Direct PVT supply mode, especially at the end of each night, when the
514 temperature difference between the indoor and outdoor was greater.

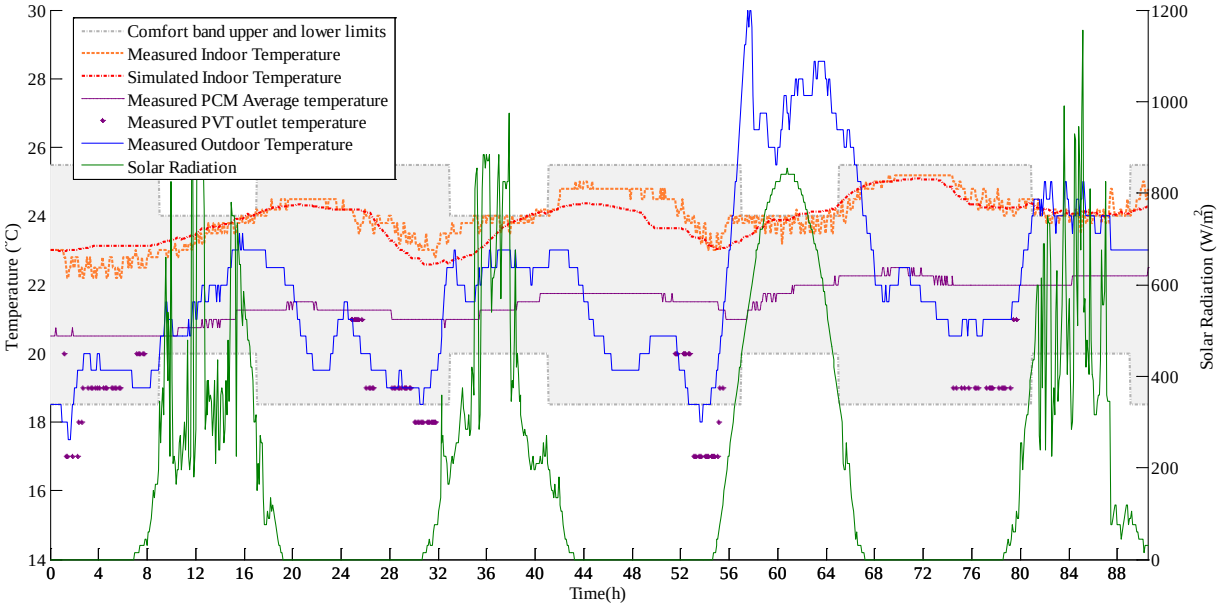

Figure 10: HMPC experimental test compared to the simulated test, HVAC only, March 2015: Temperature profiles and solar radiation.

When the pre-cooling provided by the PVT was not sufficient, the discharging of the PCM unit and the normal air conditioner were compensating to keep the temperature inside the comfort band. The profile of the activation of the various operating modes coinciding with the activation of the three low-level controllers is presented in Figure 11. In this case it is noticeable that both controllers tried to achieve their objectives with a similar sequence of the selected operating modes with night time PVT Direct pre-cooling followed by a combination of PCM Discharging and Normal Conditioning during the daytime.

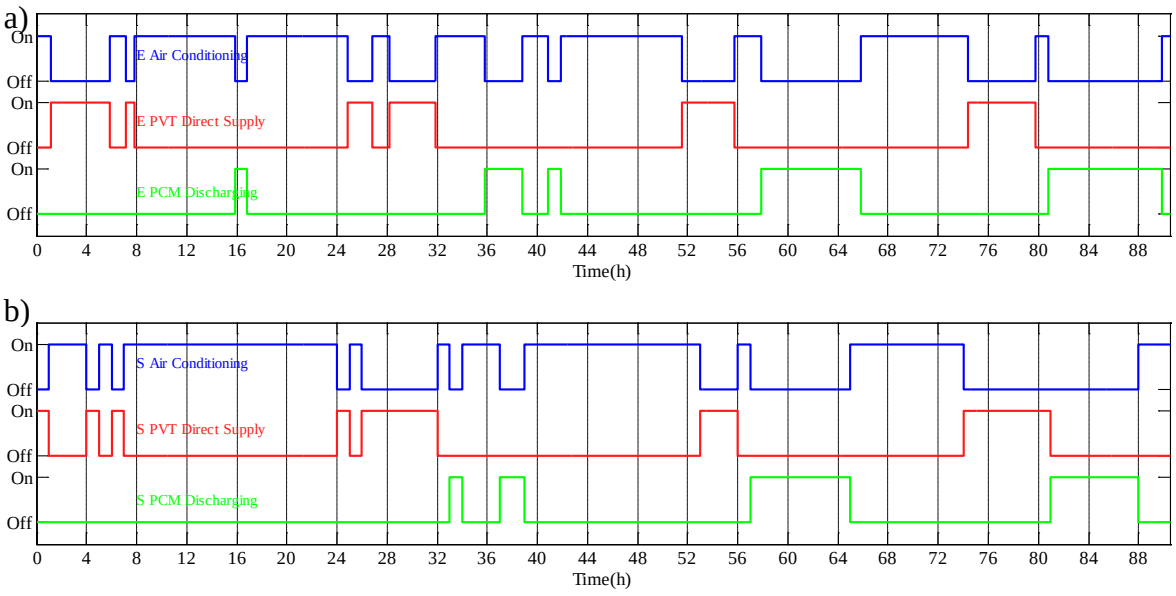

Figure 11: HMPC experimental test compared to the simulated test, HVAC only, March 2015: a) experimental and b) simulated test operating mode selection.

During the experimental test, the HVAC system provided a total of 45.2 kWh of cooling to the building, among which 14.9 kWh was from the PVT Direct Supply, 4.7 kWh was from the PCM Discharging and 25.6 kWh was from the use of the air conditioning unit. The average COP of the PVT system over the whole test, defined as the cooling provided divided by the electrical energy used by the fan, was 5.04, and the average COP of the PCM Discharging was 4.48. In both cases, the controller can maintain the performance above the reference COP of the air conditioning system, identified to be 2.1 on average.

The simulated test generated the similar results, with a total of 41.2 kWh of cooling provided to the building, among which the cooling provided the PVT, PCM unit and the air conditioning unit was 13.9, 4.7 and 22.6 kWh, respectively. The COP of the PVT system and the PCM unit discharging was 4.59 and 4.55 respectively, higher than the reference COP.

The instantaneous experimental and simulated cooling generation and COP of the various operating modes are presented in Figure 12.

It can be seen that the cooling of the house by both the PVT and PCM occurred in the similar ways in the experimental and the simulated tests, keeping the instantaneous COP of the system well above the given reference.

a)

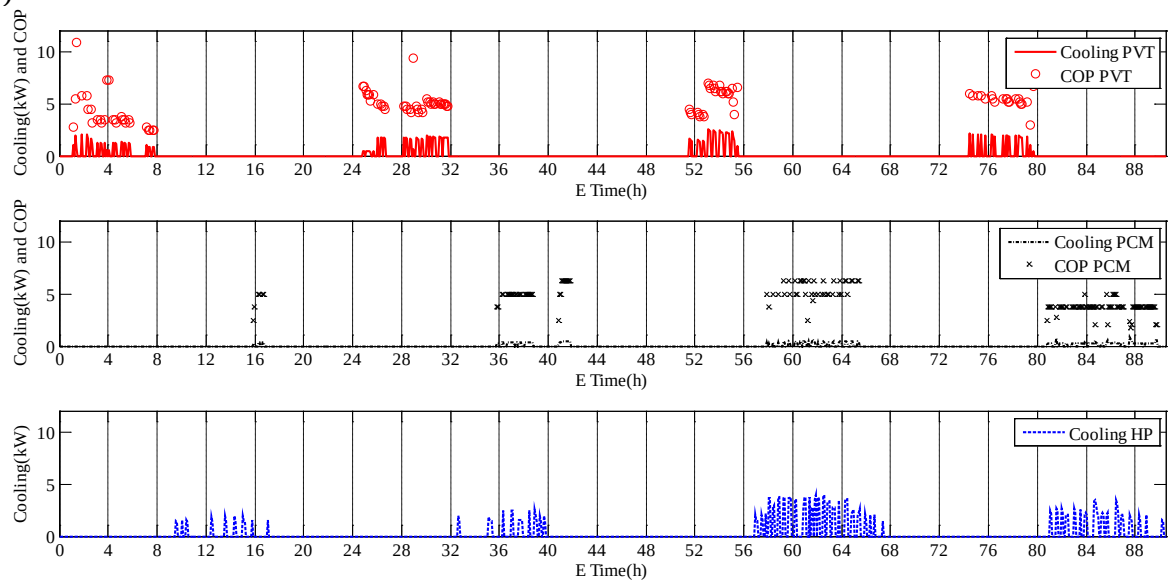

b)

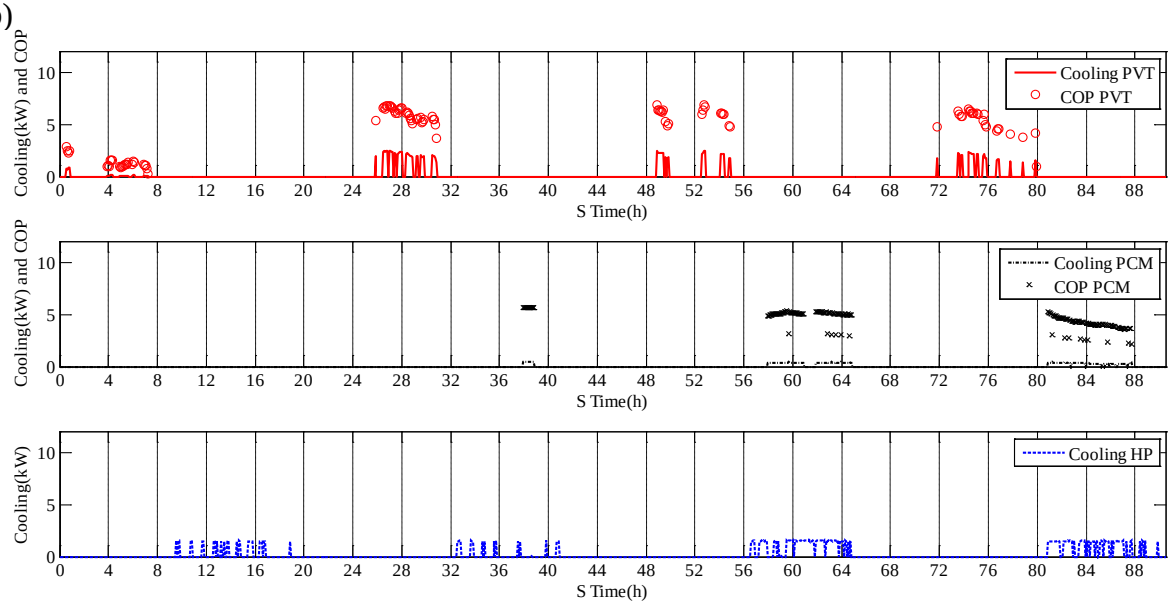

Figure 12: HMPC experimental test compared to the simulated test, HVAC only, March 2015: a) experimental and b) simulated instantaneous cooling generation and COP.

The overall performance of the experimental and simulated tests are also summarised in Table 3.

Table 3: Summary of the HVAC average performance, HMPC experimental and simulated test, HVAC only, March 2015.

	Experimental	Simulated	Relative difference
PVT Direct (kWh/day)	3.97	3.71	6.5%
Average COP PVT Direct	5.04	4.59	8.9%
PCM Discharge (kWh/day)	1.25	1.25	0.0%
Average COP PCM Discharge	4.48	4.55	1.6%
Normal Conditioning (kWh/day)	6.82	6.03	11.6%
Total Electrical Consumption (kWh/day)	4.74	4.23	10.8%

6.2 Cooling Test - Mechanical and Natural Ventilation

A similar experiment was undertaken, using both the HVAC system and natural ventilation between 14th and the 16th of April 2015. The cost associated with the windows opening was very small so that their operation was the most preferable conditioning solution for the controller to meet the thermal comfort targets, without using them if not necessary and the house can stay in the comfort band free-running with the windows closed.

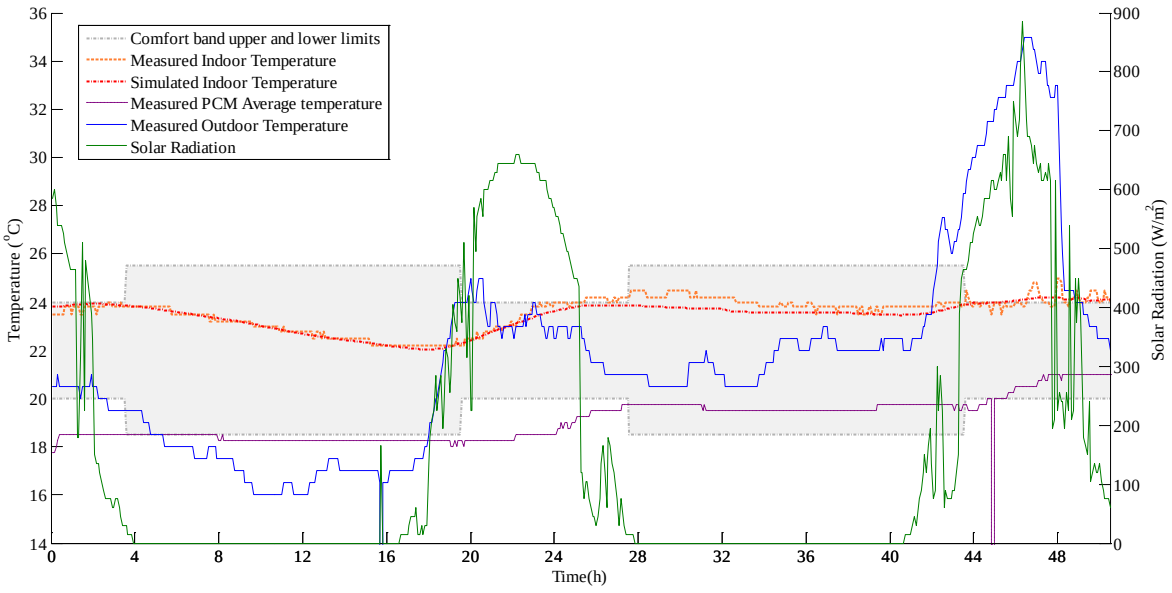

Figure 13: HMPC experimental test compared to the simulated test, HVAC and Natural Ventilation, April 2015: Temperature profiles and solar radiation.

The experimental and simulated indoor temperature profiles, outdoor temperature, global horizontal radiation and the objective temperature range are presented in Figure 13. It was be found that the simulated and the experimental trajectories were similar and the controller was

capable to effectively manage the indoor temperature even in very hot conditions. Compared to the case where only the HVAC system was used, the Low-level Controller 3 was more frequently used, since it is associated to both normal conditioning and natural ventilation modes. The possibility to cool the building using natural ventilation was preferred by the controller, since the cost associated to this mode is negligible compared to the other cooling means. This behaviour of the controller can be observed in Figure 14 noting that mostly used mode was Normal Conditioning and Natural Ventilation, by both the simulated and experimental controllers. During this test PCM Discharging mode was only utilised at the end of the second day (hours from 24 to 27) and during the third day (hours from 43 to 50). The small difference between experimental and simulated operation is mostly due to a mismatch between the model and the real system, and the need to correct the trajectory to keep the temperature in the comfort band. The simulated controller activated the PVT direct supply for a small portion of time at the end of the second night, whereas the experimental one used natural ventilation, achieving a similar result in terms of remaining in the comfort band. It can also be noted that this difference in operation is minimal if the results in Figure 15 are observed, since a very small amount of cooling was provided via the Direct PVT mode.

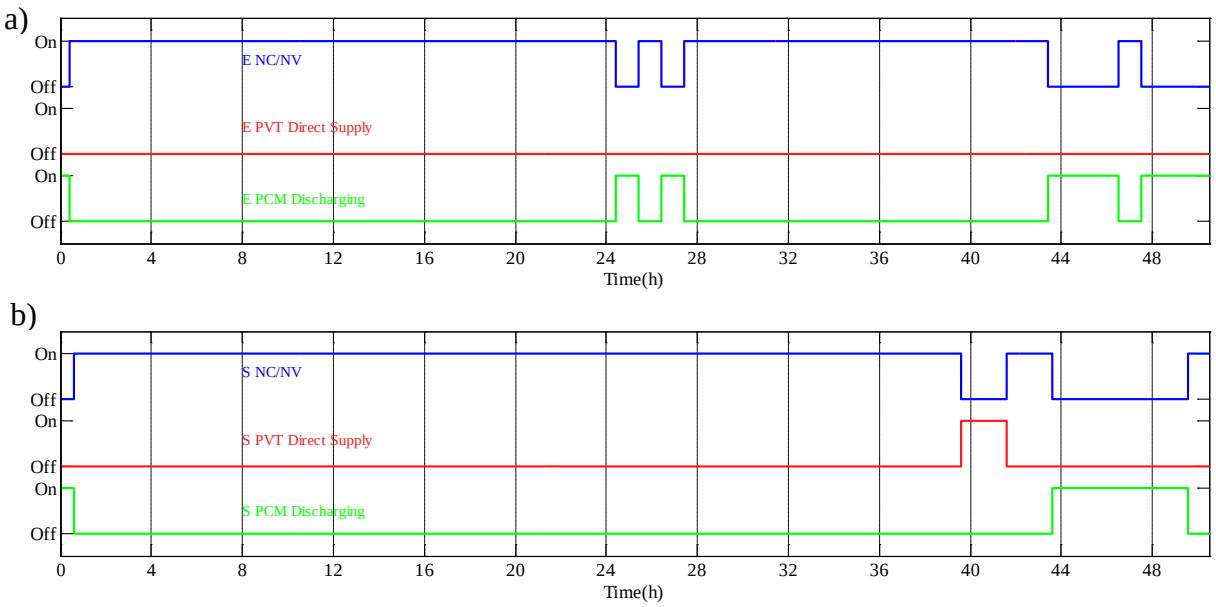

Figure 14: HMPC experimental test compared to simulated test, HVAC and Natural Ventilation, April 2015: a) experimental and b) simulated test operating mode selection.

During the experimental test the HVAC system provided a total of 12.9 kWh of cooling to the building, among which 4.9 kWh was provided by discharging the PCM unit (at an average COP of 7.1) and 8.0 kWh was supplied by using the air conditioning unit. Direct PVT mode was not used in the test. The natural ventilation mode kept the operable windows open for a total of 76 five minute control steps (i.e. 6 hours and 20 minutes) over the whole test (i.e. 50 hours and 30 minutes).

In the simulated test, the HVAC system provided 11.9 kWh of cooling, among which 0.2 kWh was from Direct PVT mode (at an average COP of 3.1), 3.2 kWh was supplied by discharging the PCM unit (at an average COP of 5.5), and 8.5 kWh was provided by using the air conditioning unit. During this simulated test, the Natural Ventilation mode was active for 99 five minute control steps (8 hours and 15 minutes).The instantaneous experimental and simulated cooling generation and COP under the various operating modes are presented in Figure 15.

In this case, the experimental and simulated test resulted in a similar pattern in the utilisation of the various resources. Natural Ventilation mode was often used during the night and

during the day when the temperature was below the current indoor average temperature (e.g. around hour 24). Both of the tests utilised PCM discharging during the last hot day, but it was also utilised in the experimental test between hour 24 and hour 28 to correct the indoor temperature trajectory.

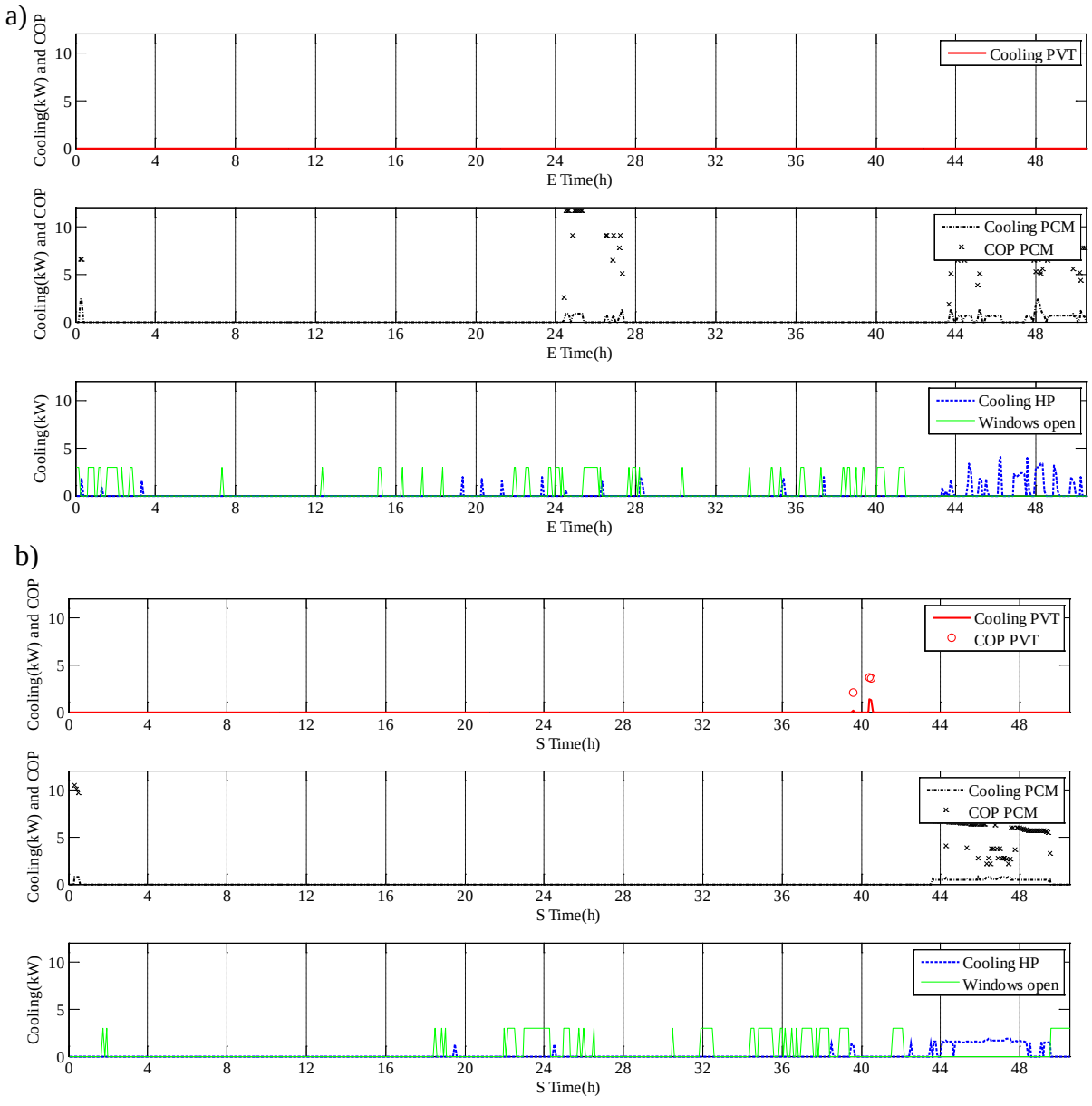

Figure 15: HMPC experimental test compared to the simulated test, HVAC and Natural Ventilation, April 2015: a) experimental and b) simulated instantaneous cooling generation and COP.

The summary of the performance of the system in the experimental and simulated tests is presented in Table 4.

610 Table 4: Summary of the HVAC average performance, HMPC experimental and simulated test,
611 HVAC and Natural Ventilation, April 2015.

	Experimental	Simulated	Relative difference
PVT Direct (kWh/day)	0	0.10	-
Average COP PVT Direct	0	3.10	-
PCM Discharge (kWh/day)	2.35	1.54	34.5%
Average COP PCM Discharge	7.10	5.50	22.5%
Normal Conditioning (kWh/day)	3.84	4.08	6.3%
Total Electrical Consumption (kWh/day)	2.15	2.17	0.9%

612

613 **7 Conclusions**

614 This paper proposed a Hybrid Model Predictive Control (HMPC) strategy to manage a solar-
615 assisted HVAC system, retrofitted to a residential building. The system features a
616 Photovoltaic-Thermal (PVT) system and a phase change material (PCM) active storage unit,
617 integrated with a standard ducted air conditioning system. Comprehensive experimental
618 control infrastructure was designed, installed and commissioned in the Illawarra Flame
619 house, allowing the implementation of virtually any typology of control strategies to the
620 house system. An HMPC strategy with two levels of control was designed, implemented and
621 its operation demonstrated through both simulations and experiments. To understand the
622 effect of the mismatch between the models and the real system, the controller was simulated
623 using an identical model for both the controller and the system while introducing the same
624 error in the weather forecast.

625 The HMPC strategy shows an anticipative behaviour that could be noticed in the cooling
626 scenarios presented in this paper, where the HMPC pre-cooled the building utilising the fact
627 that bringing fresh air further cooled by the PVT system can lower the temperature of the
628 indoor air and building fabric more efficiently than the heat pump. The HMPC strategy also
629 demonstrated the value of using natural ventilation in both the experimental tests and

simulated environment, by giving priority to window opening for cooling purposes whenever available.

The controller was able to keep the indoor temperature within the prescribed range, utilising the PVT and PCM storage to generate cooling at a higher COP than the reference standard air conditioner. The winter experiments highlighted the fact that appropriate insulation of an active PCM unit is crucial. Excessive heat losses prevented the system operated with efficient charging and discharging cycles.

Overall, the HMPC strategy demonstrated to be capable of effectively utilising the knowledge of the system future dynamics allowing it to manage well the available resources to maximise the efficiency of the system. The results presented in this paper show that the methodology proposed is implementable and promising. An important advantage of MPC techniques is that they enable the use of real-time measurements and forecasts to optimise the system performance when confronted with changing conditions and disturbances, which is particularly important when solar-driven generation is implemented on site and is only available at certain times of the day.

Acknowledgements

The authors would like to thank Prof. Alberto Bemporad and Dr. Daniele Bernardini for their advice and help in the formulation of the control problem and its implementation in the Hybrid Toolbox.

References

[1] Kolokotsa D, Rovas D, Kosmatopoulos E, Kalaitzakis K. A roadmap towards intelligent net zero- and positive-energy buildings. Sol Energy 2011;85:3067–84. doi:10.1016/j.solener.2010.09.001.

[2] Mills E. Building Commissioning: A Golden Opportunity for Reducing Energy Costs and Greenhouse Gas Emissions. 2009.

[3] Lu Y, Wang S, Shan K. Design optimization and optimal control of grid-connected

and standalone nearly/net zero energy buildings. Appl Energy 2015;155:463–77. doi:10.1016/j.apenergy.2015.06.007.

[4] ASHRAE. 2013 ASHRAE Handbook - Fundamentals (SI Edition). American Society of Heating, Refrigerating and Air-Conditioning Engineers, Inc.; 2013.

[5] ASHRAE. 2015 ASHRAE handbook - HVAC Applications. 2015. American Society of Heating, Refrigerating and Air-Conditioning Engineers, Inc..

[6] Armstrong P, Leeb S, Norford L. Control with building mass-Part I: Thermal response model. … -American Soc … 2006;112. doi:10.1016/j.apenergy.2007.08.001.

[7] Armstrong P, Leeb S, Norford L. Control with building mass-Part II: Simulation. Ashrae Trans 2006;112. doi:10.1016/j.apenergy.2007.08.001.

[8] Gwerder M, Lehmann B, Tödtli J, Dorer V, Renggli F. Control of thermally-activated building systems (TABS). Appl Energy 2008;85:565–81. doi:10.1016/j.apenergy.2007.08.001.

[9] Kim SH. An evaluation of robust controls for passive building thermal mass and mechanical thermal energy storage under uncertainty. Appl Energy 2013;111:602–23. doi:10.1016/j.apenergy.2013.05.030.

[10] Siroky J, Oldewurtel F, Cigler J, Privara S. Experimental analysis of model predictive control for an energy efficient building heating system. Appl Energy 2011;88:3079–87. doi:10.1016/j.apenergy.2011.03.009.

[11] Prívara S, Váňa Z, Žáčeková E, Cigler J. Building modeling: Selection of the most appropriate model for predictive control. Energy Build 2012;55:341–50. doi:10.1016/j.enbuild.2012.08.040.

[12] Afram A, Janabi-Sharifi F. Gray-box modeling and validation of residential HVAC system for control system design. Appl Energy 2015;137:134–50. doi:10.1016/j.apenergy.2014.10.026.

[13] Bacher P, Madsen H. Identifying suitable models for the heat dynamics of buildings. Energy Build 2011;43:1511–22. doi:10.1016/j.enbuild.2011.02.005.

[14] Malisani P, Chaplais F, Petit N, Feldmann D. Thermal building model identification using time-scaled identification methods. 49th IEEE Conf Decis Control 2010:308–15. doi:10.1109/CDC.2010.5717975.

[15] Privara S, Vana Z, Gyalistras D, Cigler J, Sagerschnig C, Morari M, et al. Modeling and identification of a large multi-zone office building. 2011 IEEE Int Conf Control Appl 2011:55–60. doi:10.1109/CCA.2011.6044402.

[16] Zacekova E, Privara S, Vana Z. Model predictive control relevant identification using partial least squares for building modeling. Aust Control Conf (AUCC), 2011 2011:422–7.

[17] Zhao Y, Lu Y, Yan C, Wang S. MPC-based optimal scheduling of grid-connected low energy buildings with thermal energy storages. Energy Build 2015;86:415–26. doi:10.1016/j.enbuild.2014.10.019.

[18] Lu Y, Wang S, Sun Y, Yan C. Optimal scheduling of buildings with energy generation and thermal energy storage under dynamic electricity pricing using mixed-integer nonlinear programming. Appl Energy 2015;147:49–58.

doi:10.1016/j.apenergy.2015.02.060.

[19] Kashima T, Boyd SP. Cost optimal operation of thermal energy storage system with real-time prices. 2013 Int Conf Control Autom Inf Sci ICCAIS 2013 2013:233–7. doi:10.1109/ICCAIS.2013.6720560.

[20] Touretzky CR, Baldea M. Integrating scheduling and control for economic MPC of buildings with energy storage. J Process Control 2014;24:1292–300. doi:10.1016/j.jprocont.2014.04.015.

[21] Berkenkamp F, Gwerder M. Hybrid model predictive control of stratified thermal storages in buildings. Energy Build 2014;84:233–40. doi:10.1016/j.enbuild.2014.07.052.

[22] Rodriguez M, De Prada C, Capraro F, Cristea S, De Keyser R. Hybrid Predictive Control of a Solar Air Conditioning Plant. Eur J Control 2008:1–15. doi:10.3166/EJC.14.1.

[23] Siroky J. Hybrid MPC approach to reconfiguration of building heating system. Eur Control Conf 2013:2675–80.

[24] Lindel D, Afshari H, Alisafaee M, Biswas J, Caban M, Mocellin X, et al. Field tests of an adaptive, model-predictive heating controller for residential buildings. Energy Build 2015;99:292–302. doi:10.1016/j.enbuild.2015.04.029.

[25] Di Giorgio A, Liberati F. Near real time load shifting control for residential electricity prosumers under designed and market indexed pricing models. Appl Energy 2014;128:119–32. doi:10.1016/j.apenergy.2014.04.032.

[26] Fiorentini M, Cooper P, Ma Z, Robinson DA. Hybrid model predictive control of a residential HVAC system with PVT energy generation and PCM thermal storage. Energy Procedia 2015;83:21–30. doi:10.1016/j.egypro.2015.12.192.

[27] Bemporad A, Morari M. Control of systems integrating logic, dynamics, and constraints. Automatica 1999;35:407–27. doi:10.1016/S0005-1098(98)00178-2.

[28] Bemporad A. Hybrid Toolbox User ' s Guide 2012: Available at: http://cse.lab.imtlucca.it/~bemporad/hybrid/toolbox/.

[29] Fiorentini M, Cooper P, Ma Z. Development and optimization of an innovative HVAC system with integrated PVT and PCM thermal storage for a net-zero energy retrofitted house. Energy Build 2015;94:21–32. doi:10.1016/j.enbuild.2015.02.018.

[30] OASIS. oBIX 2015. http://www.obix.org/ (accessed August 28, 2015).

[31] Gurobi. Available at: http://www.gurobi.com/ (accessed August 28, 2015).

[32] Mathworks. Matlab System Identification Toolbox 2015.

[33] Ljung L. Ljung L System Identification Theory for User.pdf. PTR Prentice Hall Up Saddle River NJ 1987;25:475–6. doi:10.1016/0005-1098(89)90019-8.

[34] PCM Products. Available at: http://www.pcmproducts.net/ [Accessed August 28, 2015].

[35] Fiorentini M, Cooper P. Experimental Investigation of an Innovative HVAC System with Integrated PVT and PCM Thermal Storage for a Net-Zero Energy Retrofitted House. ASHRAE Winter Confrence, Chicago, 2015.

739 [36] Bemporad A. Model predictive control design: New trends and tools. Proc 45Th Ieee
740 Conf Decis Control Vols 1-14 2006:6678–83. doi:10.1109/CDC.2006.377490.

741 [37] Ren MJ, Wright J a. Adaptive Diurnal Prediction of Ambient Dry-Bulb Temperature
742 and Solar Radiation. HVAC&R Res 2002;8:383–401.
743 doi:10.1080/10789669.2002.10391297.

744

745